Engineering Notes

Interface Thermal Conductance in a Vacuum

ERWIN FRIED*
General Electric Company, King of Prussia, Pa.
AND
HARRY L. ATKINS†
NASA Marshall Space Flight Center, Huntsville, Ala.

THE thermal joint conductance between metallic surfaces in a vacuum has recently become of considerable interest in a number of fields where the transfer of heat between mating surfaces must be accomplished in the absence of a conducting fluid. The most prominent of these applications include space vehicles with their environmental control subsystems and space-vehicle energy-conversion devices. This note presents the results to date of a primarily experimental study of the interface thermal contact conductance between metals in a vacuum.

Problem Statement

When two metallic surfaces are held in contact, the heat transfer between them is a function of the actual contact area, the interstitial fluid, and the thermal properties of the contact surfaces. The actual contact area for nominally flat surfaces, in turn, is a function of the contact pressure, the surface conditions, the elastic and plastic properties of the material, and, at low and moderate contact pressure, the degree of surface mating. For the case of the thermal contact conductance in a vacuum, the predominant mode of heat transfer is through the asperities making up the actual contact points, since, at gas pressures of 10^{-2} newton/m^2 (10^{-4} mm Hg), the free molecule conductivity in the gap represents less than 1% of the thermal conductivity at normal temperature and pressure.

The thermal contact conductance is defined as $h_c = Q/(A\Delta T)$, where Q is the heat flow rate through the contact, A is the apparent area of the contact (i.e., the projected area of the contact perpendicular to the direction of heat flow), and ΔT is the additional temperature drop due to the interface.

The modes of heat transfer to be considered are: thermal radiation, molecular or other conduction through the interstitial fluid, and solid conduction through the asperities. These three heat-transfer modes are interdependent and should be treated as such. For contacts in vacuum, as this study indicated, solid conduction through the asperities represents the most significant part of the heat-transfer mechanism for all but very low contact pressures. For a detailed discussion of the foregoing, the reader is referred to Refs. 1–4, which cover the subject adequately.

Experimental Program

An experimental program was undertaken to aid in understanding the heat-transfer mechanism, provide data to verify existing prediction techniques, and provide data to aid in the development of improved techniques for the analysis of thermal contact conductance. To this end a thermal contact conductance apparatus suitable for use in a vacuum was developed, which would permit contact pressure variations while under vacuum. A schematic of this test apparatus is shown in Fig. 1.

Test samples consisted of two metallic cylinders having a diameter of 5.08 cm (2 in.) and a length of 7.62 cm (3 in.) each. Each sample was instrumented with four copper-constantan thermocouples to determine the axial temperature gradient due to the uniform heat flux passing between the electric heater and the liquid-cooled sink. Contact pressure could be varied by means of a stainless-steel bellows, pressurized in accordance with the desired load, which, in turn, was measured using a strain gage load washer on the heat sink side. The entire assembly was installed in a bell-jar vacuum system with a right-angle cold trap, utilizing a 4-in. oil-diffusion pump to achieve a vacuum of 10^{-4} torr or better.

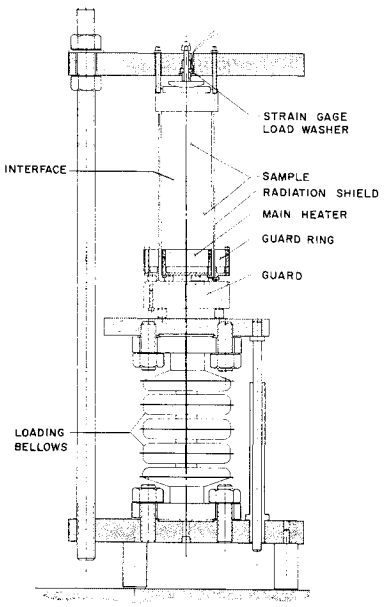

Fig. 1 Test apparatus schematic.

The heat source utilized in this test was a 100-w electric-resistance element embedded in the main heater assembly, which is guarded by a ring heater and a rear guard heater, as shown in Fig. 1. This system is arranged so that there exists no significant temperature difference between the main heater and the guards. Each is controlled separately so that all thermal energy from the main heater has only one direction to go: into the test sample. The heat flux was determined by measuring the regulated d.c. power input, i.e., voltage and current, using precision instruments. In order to monitor potential radiation errors in this system, sufficient thermocouples were fastened to the several surfaces seeing each other.

The temperature difference ΔT, used in the conductance equation, is based on the temperatures obtained experimentally, which are then extrapolated to the interface. The accuracy with which this ΔT can be obtained is a function of the accuracy with which the temperature gradient in the sample can be obtained. For high values of contact conductances, the ΔT usually was quite low; conversely, for low values of conductance, the ΔT was high.

Presented at 1st AIAA Annual Meeting, Washington, D. C., June 29–July 2, 1964; revision received January 8, 1965. This work was carried out under NASA Contract No. NAS8-5207, Research Projects Laboratory, Marshall Space Flight Center, Huntsville, Ala.

* Consulting Engineer, Thermal Technologies. Member AIAA.
† Physicist.

Table 1 Sample materials tested

Sample no.	Material	Rockwell hardness	Maximum flatness deviation, μm
1	Stainless steel 304[a]	B-80	−1.3
2	Stainless steel 304[a]	B-80	...
3	Stainless steel 304[a]	B-80	−1.3
4	Stainless steel 304[a]	B-81	+2.5
7	AZ-31B magnesium	E-63	−1.3
8	AZ-31B magnesium	E-61	−7.6
9	AZ-31B magnesium	E-62	−5.1
10	AZ-31B magnesium	E-62	−3.8
13	6061-T6 aluminum	F-88	...
14	6061-T6 aluminum	F-87	−1.3
15	6061-T6 aluminum	F-93	+6.4
16	6061-T6 aluminum	F-93	+2.5
25	Oxygen free high cond. copper	B-48	+6.4
26	Oxygen free high cond. copper	B-48	+1.3
27	ARMCO iron		

[a] Ground finish, all others lathe cut.

Considerable attention was paid to accurate temperature-measurement techniques in order to minimize possible measurement errors, since the quality of the temperature measurement directly affected the quality of the interface thermal contact conductance obtained. Thermocouple junctions were made of 30-gage copper-constantan precision-grade thermocouple wire and were installed in the test samples in 2.54-cm-deep holes, to place the junction at the cylinder axis. The junction was embedded with Eccobond 56C, an epoxy base cement having a thermal conductivity close to that of stainless steel. Particular attention was paid to the precision with which the axial distances between thermocouples were controlled, since the axial distance vs temperature plots were used to project the temperature gradients to the interface and thus obtain the interface temperature difference.

The constriction resistance effects at and near the interfaces require that thermocouples be located in the undisturbed region in order to correctly project the temperature gradient. Since only the sample-half interfaces are of interest, the heat source and heat sink interfaces with the samples had high vacuum silicone grease applied as a heat-transfer promoting device. Thus, no significant constriction effects resulted at the interfaces adjacent to the heat source and heat sink. However, such constriction effects were noted for thermocouples located $\frac{1}{4}$ in. (0.63 cm) from the test interface.

One significant parameter, which strongly affects the thermal contact resistance, is the surface finish of the interface. Surface finish, by definition, can include surface roughness as well as waviness or flatness. A Taylor-Hobson "Talysurf" stylus-type profilometer was used to obtain single-line profiles, as well as roughness readings of the various surface finishes prepared for this program. Flatness measurements

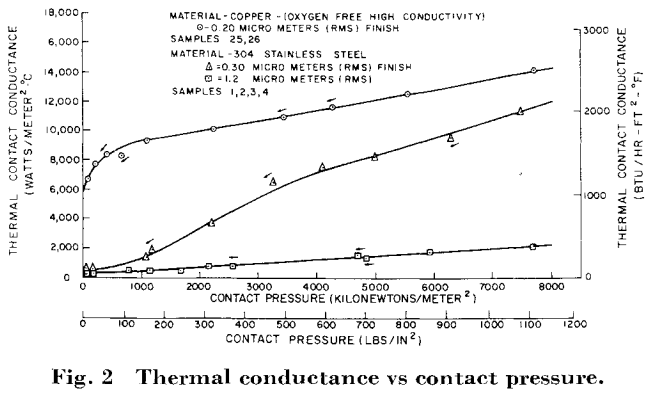

Fig. 2 Thermal conductance vs contact pressure.

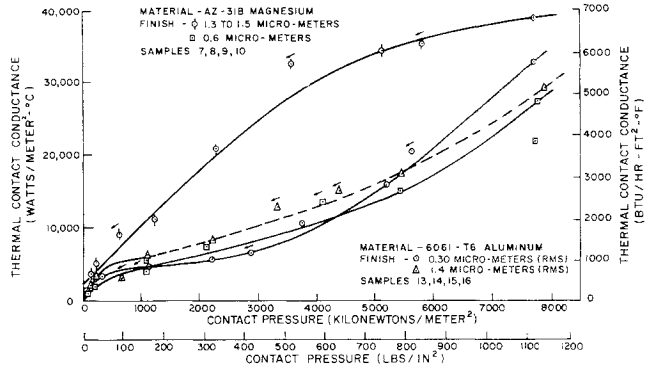

Fig. 3 Thermal conductance vs contact pressure.

were made using a surface plate and a dial indicator reading with divisions of 2.5 μm (10^{-4} in.), which permitted estimation of half divisions (1.3 μm). The maximum flatness deviation, thus obtained, represents the maximum departure of surface points from a best-fit plane through the center of the test surface. Table 1 shows the surfaces measured.

Experimental Results

Stainless steel 304

Data for a stainless-steel specimen is shown in Fig. 2 and indicates the relative effect of surface finish. Although both sample pairs had a ground test interface, they differed primarily in roughness and flatness. The much higher conductance curve of the 0.3-μm-finish sample with a slightly better flatness also indicates some hysteresis in the loading-unloading sequence. The coarse finish sample shows no such hysteresis. The results shown are quite similar to those of Clausing.[2]

OFHC copper

A contact conductance test for high-purity copper was carried out, because no such data existed in the literature, except that of Jacobs and Starr[6] for low contact pressure. Their data indicated a linear variation of conductance with load which does not conform to experience with other metals. As can be seen in Fig. 2, the obtained curve in this experiment is not linear at low loads, but does show linearity at higher loads. It is also of interest that no hysteresis was observed for this relatively poor flatness (7.7×10^{-6}m), fine lathe finish test sample.

6061-T6 aluminum

The data shown in Fig. 3 is of interest because it shows no significant differences between the conductance of fine and coarse finish test samples. No plausible explanation can be given at present for this similarity, since the differences in surface finish, as well as flatness deviations, should have made the fine finished sample curve much better. The range of the data agrees with that of other investigators.

AZ-31-B magnesium

The test results for this material (Fig. 3) show an interesting reversal of expected conductances. These samples, which had lathe-turned interfaces, exhibited higher conductance values for the coarse finish (1.4 μm) than for the finer finish surfaces. One possible explanation would be the possible deleterious effect of oxide films on the surface finish. Since a coarse finish has fewer ridges along the asperities, the higher load per unit area could cause the film to rupture and expose more metal, thus resulting in larger constant area and better conductance. Oxide films and tarnish were evident on both sample pairs, since more than two months had elapsed between machining and test.

Conclusions

This study presents experimental results, which are in substantial agreement with results obtained by other investigators for similar materials. One possible explanation for the character of the conductance curves may be due to the sequence of achieving the surface areas contacting each other. Initially, only one or more discrete areas are in contact. As load is applied and the surfaces deform, the contact areas increase, and new regions make contacts. Since this is not a rigorously predictable or controllable process for engineering-type surfaces, as opposed, for example, to the sphericity of the contact surfaces of Clausing,[2] the prediction of the contact conductances becomes difficult. Although several investigators have developed theoretical analyses of this problem, they have been able to predict the thermal contact conductance for specialized conditions and surfaces only. At this time, there are no suitable theoretical analyses available which apply to the general case, although a need exists for such analyses and prediction methods.

References

[1] Fried, E. and Costello, F. A., "Interface thermal contact resistance problem in space vehicles," ARS J. **32**, 237–243 (1962).

[2] Clausing, A. M. and Chao, B. T., "Thermal contact resistance in a vacuum environment," American Society of Mechanical Engineers Paper 64-HT16 (1964); also J. Heat Transfer (to be published).

[3] Fenech, H. and Rohsenow, W. M., "Prediction of thermal conductance of metallic surfaces in contact," J. Heat Transfer **85**, 15–24 (February 1963).

[4] Holm, R., *Electrical Contacts Handbook* (Springer-Verlag, Berlin, 1958), 3rd ed.

[5] Atkins, H. and Fried, E., "Thermal interface conductance in a vacuum," AIAA Preprint 64-253 (June 1964).

[6] Jacobs, R. B. and Starr, C., "Thermal conductance of metallic contacts," Rev. Sci. Instr. **10**, 40 (1939).

Need for a Variable Burning-Rate Solid Propellant

GERALD GOLUB*
Martin Company, Orlando, Fla.

AT the present time, a large amount of work is being done to increase the specific impulse of solid propellants. However, some of these higher-specific-impulse propellants (e.g., recently developed composite propellants utilizing nitronium or hydrazine perchlorate) are ruled out for many applications because of their handling and storage properties.

Table 1 Typical solid-propellant applications

Application	Burning rate,[4] in./sec
Booster	1–10
Sustainer	0.2–1.0
Gas generator	0.01–0.2
Sounding	0.05–0.5
Ejection	1–10
Vernier	0.5–5.0
Separation	1–10
Retro-units	1–10
Spin	1–10
Space applications	0.05–5.0

Presented as Preprint 64-372 at the 1st AIAA Annual Meeting, Washington, D. C., June 29–July 1, 1964; revision received September 14, 1964.

* Design Engineer, Propulsion Section.

Table 2 Binder materials for solid propellants

Polyurethane	Nitrocellulose—nitroglycerin
Polybutadiene-acrylic acid	Styrene
Polysulfide	Alkyd resin
Cellulose acetate	Carbonyl polyester
Butadiene	Petrin acrylate
Methyl vinylpyridine	Acrylonitrile
Polyisobutylene	Polyvinyl chloride
Isoprene	Polyepoxide
Methoxyethyl acrylate	Polyacrylamide
Methyl acrylate	Asphalt

In other cases, the specific-impulse gain is sacrificed when the propellant burning rate is altered to suit the particular engine application; such changes usually require a propellant development program. This situation is expensive in time and money and reduces the flexibility of the over-all system.

The propellant application survey shown in Table 1 indicates that burning rates ranging from 0.01 to 10 in./sec are required. This requirement should be met with several rather than the hundreds of formulations of fuels, oxidizers, and binders now being used. Among these three propellant components, the most variable is the binder (Table 2). Each propellant company appears to prefer certain binders and to protect its knowledge with respect to them. As the propellant industry becomes more mature, this large number of candidate systems will be reduced.

Table 3 shows present and desirable ranges of solid-propellant properties. There appear to be two classes of propellants; one has a high flame temperature to get high specific impulse and has a burning-rate requirement between 0.1 and 10 in./sec; the other has a burning-rate requirement in the range of 0.01 to 0.2 in./sec.

The more common techniques for controlling the burning rate are 1) altering the burning surface,[1–3] 2) changing the combustion chamber pressure, 3) adding burning-rate catalysts to the formulations, and 4) changing the particle size of solid ingredients, but these techniques often reduce the performance of the solid-propellant motor. Burning rate can be increased without loss in performance by using metal fuels in various forms: hollow or filled spheres, wires of various diameters, foils of various thicknesses, staples of various lengths, or various mixtures of exothermic metal alloys (Table 4). Table 5 shows increases in burning rate (r) obtained by embedding 5-mil wires of various metals in an end-burning propellant grain[4] in the longitudinal (flame propagation) direction. The thermal diffusivities (α) and melting points (m.p.) of the metals also are given in Table 5. There appears to be some correlation between r and α but no clear trend with melting point; however, other data have shown that plating a low-melting-point metal, such as silver or copper, with 1 mil of a high-melting-point metal, such as platinum, increased the propellant burning rate. Unfortunately, there is no comparably simple way to reduce burning rate without penalty. Use of encapsulated endothermic or exothermic reacting material may offer a method of varying burning rate in either direction. When burning rate is varied, the effects on formu-

Table 3 Present and desirable ranges for solid-propellant properties

Parameter	Present range	Desired range
Burning rate, in./sec at 100 psi	0.05–2.0	0.01–10
Burning time of motors 50–60 in. in diameter, sec	2.5–80	0.5–100
Density, lb/in.^{3}	0.052–0.0715	0.06–0.08
Flame temperature, °K	1200–4400	1000–5000
Number of propellant ingredients	4–15	1–3